

A Novel Magnetic Gear: Towards a Higher Torque Density

Xin Yin, *Student Member, IEEE*, Pierre-Daniel Pfister, *Member, IEEE*, and Youtong Fang, *Member, IEEE*
 College of Electrical Engineering, Zhejiang University, Hangzhou 310027, Zhejiang

Magnetic gears, a promising alternative to conventional mechanical gear boxes, have gained growing attention in the last decade. This paper proposes a novel topology of flux focusing magnetic gear which makes use of both axial and transverse magnetic fluxes. Important geometrical parameters are optimized using a sequential parametric sweeping analysis. Performances are validated by a three-dimensional finite element method and compared with existing magnetic gears. The result indicates that by reducing the saturation in soft magnetic materials and the flux leakage, the new topology has a significantly high torque density within a wide length-diameter ratio.

Index Terms—Axial flux, flux focusing, high torque density, magnetic gear, transverse flux.

I. INTRODUCTION

MAGNETIC gears (MGs) are potential alternatives to conventional mechanical gear boxes. Since MGs transmit torque or power via interaction of magnetic field without mechanical contact, they operate with less vibration, reduced acoustic noise and no lubrication except in the ball bearings. MGs also feature intrinsic overload protection by working in a slip mode, which avoids further damage to the system. In addition, seamless integration of MGs into conventional electrical machines results in a compact design with a high torque density. Because of these advantages, MGs are suitable for a variety of applications in areas such as wind turbine, electric vehicle and marine propulsion. With high performance PMs and new topologies, today MGs are capable to transmit a torque that is competitive with mechanical gear boxes [1].

In this paper, a novel axial-transverse flux magnetic gear (ATFMG) is proposed using a flux focusing technique. Important geometrical parameters are optimized using a parametric sweeping analysis. The performance is validated by a three-dimensional finite element method (3D FEM) and compared with existing MGs.

II. STATE OF THE ART

MGs can be categorized by their flux orientations, namely, radial flux magnetic gear (RFMG), axial flux magnetic gear (AFMG) and transverse flux magnetic gear (TFMG). The first high-performance coaxial magnetic gear uses a radial flux structure whose torque density was over 100 Nm/L [2]. The torque densities of the RFMGs found in the literature range from 50 Nm/L to 160 Nm/L [1]–[6]. Neglecting end effects, the torque transmission capability of a RFMG is proportional to its axial length and thus its torque density is theoretically independent of the axial length. An AFMG can offer a hermetic isolation between the input and output shafts [7]. Compared with the torque density of a RFMG, the torque density of an AFMG is higher because of a larger effective area. Nonetheless, due to the axial-flux structure, the increase in axial length contributes little to the increase in torque density. As a result, most of AFMGs take a pancake shape with

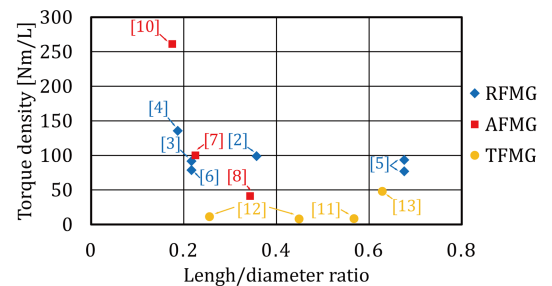


Figure 1. Simulation results of torque densities of existing MG designs with normalized high-remnance PMs and high-saturation-flux-density soft magnetic materials (Table I).

small length-diameter ratio [7]–[10]. Transverse flux electrical machines are known for their high torque density. It was hence expected that a TFMG would possess the same merit. On the contrary, the torque densities of TFMGs were relatively low [11]–[13]. There are several techniques that can improve the torque density. A RFMG using Halbach PM arrays offers 14% increase in torque density [4]. Flux focusing is another way to increase air-gap flux density and consequently, the torque density of a MG [5]. Unlike surface-mounted MGs, the PMs in flux focusing MGs are circumferentially magnetized to focus flux in the soft magnetic materials.

In order to have a quick benchmark for our work, we reviewed the torque densities of existing designs found in the literature. To reduce the influences of different materials, we selected those designs which use high-energy PMs and simulated each design using FEM with normalized high-remnance PMs and high-saturation-flux-density soft magnetic materials (Table I). The simulation results (Fig. 1) show that the RFMGs have good torque densities for different length-diameter ratios. The TFMGs show a relatively low torque density. The AFMG can have a superior torque density with a small length-diameter ratio. The highest torque density seen in Fig. 1 is from the flux-focusing AFMG in [10]. Our work starts from it to pursue an even higher torque density.

Manuscript received March 18, 2015; revised May 06, 2015. Corresponding author: P.-D. Pfister (email: pierredaniel.pfister.public@gmail.com).

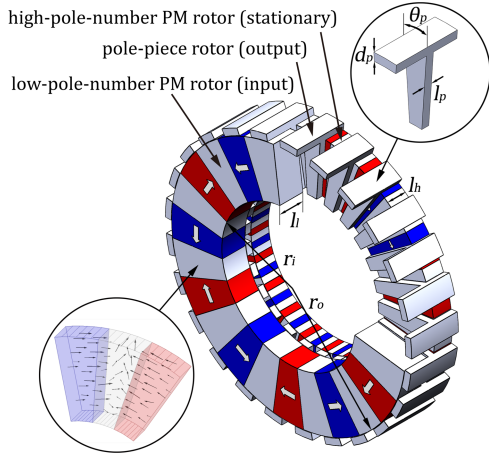


Figure 2. Schematic view of an ATFMG.

III. A NOVEL AXIAL-TRANSVERSE FLUX MAGNETIC GEAR

A. Working Principles

The considered structure of the novel ATFMG is shown in Fig. 2. The low-pole-number PM rotor (LPR) and high-pole-number PM rotor (HPR) have respectively p_l and p_h pole-pairs. The pole-piece rotor (PPR) has n_p soft magnetic pieces. Because the relationship between numbers of pole-pairs is

$$p_l + p_h = n_p, \quad (1)$$

the rotors will interact via a common space harmonic component [2]. In the proposed model, the HPR is stationary and the rotating output torque is given by the PPR. The gear ratio is

$$G_r = \frac{\Omega_l}{\Omega_p} = \frac{T_p}{T_l} = \frac{n_p}{p_l}, \quad (2)$$

where Ω_l and T_l are the angular speed and the torque of the LPR, respectively, and Ω_p and T_p are the angular speed and the torque of the PPR, respectively. PMs are circumferentially magnetized to focus flux (Fig. 2). If the arc spans of PM poles and of soft magnetic materials between them are the same, the flux focusing ratios of the LPR (C_l) and of the HPR (C_h) in an AFMG are defined in [9] as the ratio between the PM area facing the steel pole and the steel pole area facing the air gap, which are

$$C_l = \frac{8l_l p_l}{\pi(r_o + r_i)}, \quad (3a)$$

$$C_h = \frac{8l_h p_h}{\pi(r_o + r_i)}, \quad (3b)$$

where l_l and l_h are axial lengths of the LPR and the HPR, respectively, and r_o and r_i are the outer and inner radii of the two PM rotors, respectively. The magnetic flux density is increased if C_l and C_h are greater than one. The air-gap flux density of a MG using a flux focusing topology is much higher than that using a conventional surface mounted topology, resulting in a boost in torque density. Nevertheless, the air-gap flux density is limited by the saturation flux density of soft magnetic materials, which means that when the steel is highly saturated, no significant increase in the air-gap flux

Table I
FIXED GEOMETRIC PARAMETERS AND MATERIAL INFORMATION

Description	Value	Unit
Number of pole-pairs in the LPR, p_l	6	
Number of pole-pairs in the HPR, p_h	19	
Number of pole-pieces in the PPR, n_p	25	
Arc span of poles in the LPR, θ_l	15	deg
Arc span of poles in the HPR, θ_h	4.74	deg
Outer radius, r_o	140	mm
Inner radius, r_i	64	mm
Air-gap thickness, g	0.5	mm
Remanence of NdFeB permanent magnets, B_r	1.25	T
Saturation flux density of soft magnetic materials, B_s	2.1	T

Table II
SWEEPING GEOMETRICAL PARAMETERS

Description	Initial	Min.	Max.	Final	Unit
Axial length of the LPR, l_l	20	10	30	26	mm
Axial length of the HPR, l_h	15	5	25	19	mm
Axial length of the PPR, l_p	10	2	10	6	mm
Peripheral-bar thickness, d_p	5	3	13	8	mm
Arc span of pole-pieces, θ_p	5	5	10	8	deg

density will occur when the flux focusing ratio increases. Another important factor that influences the torque density of flux-focusing MGs is the flux leakage which occurs on the surfaces of the LPR and HPR that are not in front of soft magnetic pieces. Since there are no iron yokes in flux focusing MGs, the flux leakage is even more evident.

In an ATFMG, the flux focusing technique is employed here both to increase the magnetic flux density and to provide radial and axial flux orientations. Compared with a conventional AFMG, the sector-shaped soft magnetic pieces in the PPR are replaced by T-shaped ones. Thus a transverse magnetic path is created in addition to the axial magnetic path. Because there are two faces facing air gaps, the flux focusing ratios for the ATFMG become

$$C_l = \frac{8l_l p_l (r_o - r_i)}{\pi(r_o^2 - r_i^2 + 2r_o l_l)}, \quad (4a)$$

$$C_h = \frac{8l_h p_h (r_o - r_i)}{\pi(r_o^2 - r_i^2 + 2r_o l_h)}. \quad (4b)$$

The flux focusing ratios in (4) are smaller than those in (3) for identical diameters and axial lengths. Since the magnetic flux is guided axially and radially, the saturation effect is reduced without decreasing the total flux generated by PMs. Consequently, the torque density will benefit from the T-shaped design. Moreover, by adding peripheral soft magnetic bars, flux leakage on the outer lateral surfaces of the two PM rotors is significantly reduced.

B. Parametric Optimization

In this paper, the peak output torque T_o is calculated using the virtual work principle and the volume torque density τ is given by

$$\tau = \frac{T_o}{V} = \frac{T_o}{\pi r_o^2 L}, \quad (5)$$

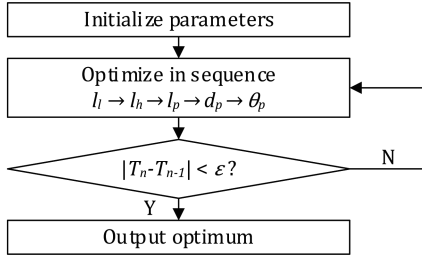


Figure 3. Flowchart of the optimization procedure.

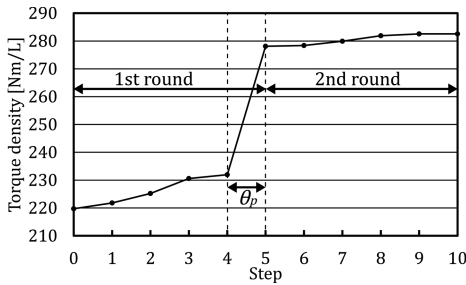


Figure 4. Evolution of the torque density after each optimizing step.

where V , r_o , and L are the volume, outer radius, and axial length of the active parts of a magnetic gear, respectively.

A parametric sweep analysis is conducted to improve the geometry of the proposed ATFMG for a higher torque density. The flowchart of optimizing procedure is shown in Fig. 3 which optimizes each parameter in sequence. The values for fixed parameters are listed in Table I. The initial value, sweeping range and optimized value for each sweeping parameter are listed in Table II. Firstly, l_l is varied while keeping other parameters constant. The result shows that when l_l is 24 mm, the torque density peaks at 221.8 Nm/L. Keeping l_l at this optimum, l_h is then changed whilst keeping other parameters constant. The torque density reaches its peak value at 225.2 Nm/L when l_h is 21 mm. In a similar way, the remaining parameters are optimized one by one in a sequence from l_l , l_h , l_p , d_p to θ_p . For further improvement, the procedure is run again from the start until no evident variation occurs. Fig. 4 shows the evolution of torque density after each step which indicates that the torque density increases from 219.74 Nm/L to 282.56 Nm/L through the optimization. In this case, the torque density increases dramatically after the fifth step due to the variation of θ_p , the pole arc of soft magnetic pieces has a significant impact on the torque transmission capability.

C. Performance

The wave form and harmonic components of magnetic flux densities generated by the LPR in the radial and axial air gaps adjacent to the HPR when the HPR is not present are shown in Fig. 5. The proposed topology differs from existing ones in that it has two magnetic paths. As shown in the Fig. 5, both axial and transverse flux densities have a dominant harmonic with the pole-pair number of 6 which is the same as that of the LPR. Another dominant harmonic has a pole-pair number of 19 which is the same as that of the HPR, resulting from modulation of the PPR. This flux modulation

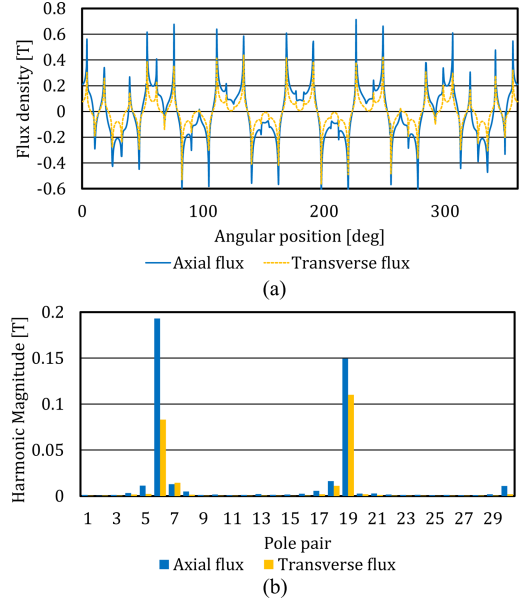


Figure 5. (a) Flux-density distributions due to LPR in the air-gap adjacent to HPR when the HPR is not present; and (b) their space harmonic spectra.

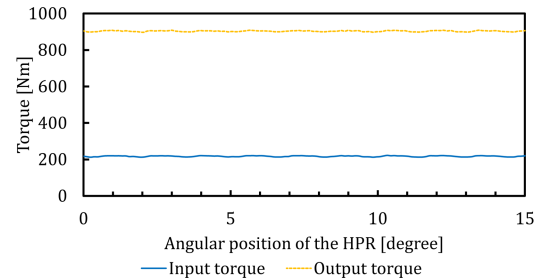


Figure 6. Input and output torques of the proposed ATFMG.

effect is the fundamental for all the coaxial MGs. Similar results are observed on the LPR side. Consequently, both axial and transverse fluxes contribute to the torque transmission.

The input and output torques of the rotating MGs are shown in Fig. 6, from which we can see that the input torque of just over 200 Nm gives an output torque as high as 900 Nm with a relatively low torque ripple (1.1% of the output torque).

IV. COMPARISON STUDY WITH AN AXIAL FLUX MAGNETIC GEAR

To validate the performance of the proposed ATFMG, we conduct a comparison study with an AFMG based on 3D FEM. A flux focusing AFMG is optimized as a benchmark using the same method as in Section III-B. The length-diameter ratio of the optimized AFMG is 0.175 and more information is listed in Table III. The resultant geometrical parameters are the same as [10]. The torque density of the optimized AFMG is 261.17 Nm/L.

Since it is more conclusive to compare both topologies with the same length-diameter ratio, a non-optimized ATFMG is then modeled with the same l_l , l_h , l_p , θ_p , g , r_o , and PM volume as the optimized AFMG. The resultant torque density is 268.4 Nm/L for the ATFMG which is higher than the

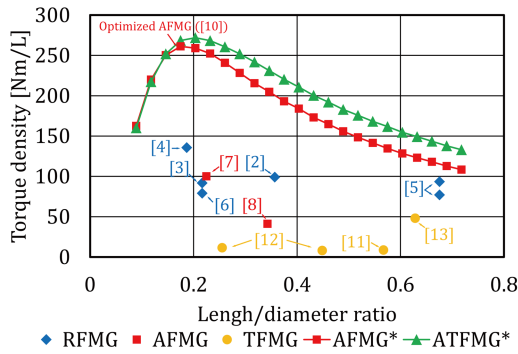


Figure 7. Comparison between torque densities of ATFMG and existing MG designs with normalized materials (* the results of the comparison study).

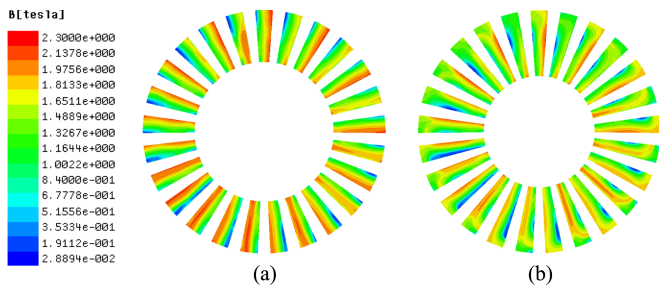


Figure 8. Cross-section view of flux distributions with the length-diameter ratio of 0.175 in (a) AFMG; (b) ATFMG.

AFMG. On the other hand, the difference of torque ripple percentages is small (1.07% for the ATFMG and 1.06% for the AFMG). To clarify the reason for the superiority of the ATFMG, we only change l_l and l_h (keeping l_l/l_h constant) of the two designs with other geometrical parameters unvaried. The result for the comparison study is plotted in Fig. 7. It shows that both structures provide a sufficiently high torque density when the length-diameter ratio is small. As l_l and l_h increase, the superiority of the ATFMG to the AFMG becomes more evident. It is because the saturation of soft magnetic materials is more severe in longer structures and it is more difficult for flux to go through the axial direction. Since T-shaped soft magnetic pieces provide an additional transverse magnetic path, the saturation effect is reduced. Magnetic flux density at cross sections in the middle of PPRs of the AFMG and the ATFMG with the length-diameter ratio of 0.175 is compared in Fig. 8, which shows clearly that the saturation in the AFMG is more severe than that in the ATFMG.

The simulation results for existing topologies with normalized materials (Table I) are also plotted in Fig. 7 for comparison. The proposed ATFMG maintains a high torque density above 150 Nm/L within a range of length-diameter ratio from 0.1 to 0.6.

V. CONCLUSION

A novel axial-transverse flux magnetic gear is proposed in this paper. Both axial and transverse fluxes are used by using T-shaped soft magnetic pieces. Therefore, the saturation of soft magnetic materials and flux leakage are reduced. The optimized ATFMG can achieve a torque density of 282.56 Nm/L. The result of comparison study indicates that the proposed

Table III
GEOMETRICAL PARAMETERS OF THE OPTIMIZED AFMG

Description	Value	Unit
Number of pole-pairs in the LPR, p_l	6	
Number of pole-pairs in the HPR, p_h	19	
Number of pole-pieces in the PPR, n_p	25	
Arc span of poles in the LPR, θ_l	15	deg
Arc span of poles in the HPR, θ_h	4.74	deg
Outer radius, r_o	140	mm
Inner radius, r_i	80	mm
Air-gap thickness, g	0.5	mm
Axial length of the LPR, l_l	25	mm
Axial length of the HPR, l_h	15	mm
Axial length of the PPR, l_p	8	mm
Arc span of pole-pieces, θ_p	8.5	deg

ATFMG has a significantly higher torque density than existing topologies within a wide range of length-diameter ratio.

ACKNOWLEDGMENT

This work was supported in part by the National Natural Science Foundation of China (51450110078, U1434202, and 51177144), the Fundamental Research Funds for the Central Universities (2015QNA4019), and the National High Technology Research and Development Program of China (2011AA11A101).

REFERENCES

- [1] E. Gouda, S. Mezani, L. Baghli, and A. Rezzoug, "Comparative study between mechanical and magnetic planetary gears," *Magnetics, IEEE Transactions on*, vol. 47, no. 2, pp. 439–450, Feb 2011.
- [2] K. Atallah and D. Howe, "A novel high-performance magnetic gear," *Magnetics, IEEE Transactions on*, vol. 37, no. 4, pp. 2844–2846, 2001.
- [3] P. Rasmussen, T. Andersen, F. Jorgensen, and O. Nielsen, "Development of a high-performance magnetic gear," *Industry Applications, IEEE Transactions on*, vol. 41, no. 3, pp. 764–770, May 2005.
- [4] L. Jian, K. Chau, Y. Gong, J. Jiang, C. Yu, and W. Li, "Comparison of coaxial magnetic gears with different topologies," *Magnetics, IEEE Transactions on*, vol. 45, no. 10, pp. 4526–4529, Oct 2009.
- [5] X. Li, K. Chau, M. Cheng, W. Hua, and Y. Du, "An improved coaxial magnetic gear using flux focusing," in *Electrical Machines and Systems (ICEMS), 2011 International Conference on*, Aug 2011, pp. 1–4.
- [6] N. Frank and H. Toliyat, "Analysis of the concentric planetary magnetic gear with strengthened stator and interior permanent magnet inner rotor," *Industry Applications, IEEE Transactions on*, vol. 47, no. 4, pp. 1652–1660, July 2011.
- [7] S. Mezani, K. Atallah, and D. Howe, "A high-performance axial-field magnetic gear," *Journal of Applied Physics*, vol. 99, no. 8, pp. 08R303–08R303–3, 2006.
- [8] T. Lubin, S. Mezani, and A. Rezzoug, "Development of a 2-d analytical model for the electromagnetic computation of axial-field magnetic gears," *Magnetics, IEEE Transactions on*, vol. 49, no. 11, pp. 5507–5521, Nov 2013.
- [9] V. Acharya, J. Bird, and M. Calvin, "A flux focusing axial magnetic gear," *Magnetics, IEEE Transactions on*, vol. 49, no. 7, pp. 4092–4095, July 2013.
- [10] V. Acharya, M. Calvin, and J. Bird, "A low torque ripple flux focusing axial magnetic gear," in *Power Electronics, Machines and Drives (PEMD 2014), 7th IET International Conference on*, April 2014, pp. 1–6.
- [11] Y. Li, J.-W. Xing, K.-R. Peng, and Y.-P. Lu, "Principle and simulation analysis of a novel structure magnetic gear," in *Electrical Machines and Systems, 2008. ICEMS 2008. International Conference on*, Oct 2008, pp. 3845–3849.
- [12] Y. Li, J.-W. Xing, Y.-P. Lu, and Z.-J. Yin, "Torque analysis of a novel non-contact permanent variable transmission," *Magnetics, IEEE Transactions on*, vol. 47, no. 10, pp. 4465–4468, Oct 2011.
- [13] W. Bomela, J. Bird, and V. Acharya, "The performance of a transverse flux magnetic gear," *Magnetics, IEEE Transactions on*, vol. 50, no. 1, pp. 1–4, Jan 2014.